

Remote Perfluoroalkyl Substituents are Key to Living Aqueous Ethylene Polymerization

Manuel Schnitte, Janine S. Scholliers, Kai Riedmiller, and Stefan Mecking*

Abstract: In various nickel(II) salicylaldiminato ethylene polymerization catalysts, which are a versatile mechanistic probe for substituent effects, longer perfluoroalkyl groups exert a strong effect on catalytic activities and polymer microstructures compared to the trifluoromethyl group. This effect is accounted for by a reduced electron density on the active sites, and is also supported by electrochemical studies. Thus, β -hydride elimination, the key step of chain transfer and branching pathways, is disfavored while chain-growth rates are enhanced. This enhancement occurs to an extent that enables living polymerizations in aqueous systems to afford ultra-high-molecular-weight polyethylene for various chelating salicylaldimine motifs. These findings are mechanistically instructive as well as practically useful for illustrating the potential of perfluoroalkyl groups in catalyst design.

Introduction

The properties of molecular catalysts are often controlled by substituents chosen to the purpose. Perfluorinated alkyl groups, $(CF_2)_nCF_3$, are well-established groups used to adjust the solubility of homogeneous catalysts.^[1] They can enhance catalysts' lipophilicity and facilitate reactions under either very apolar reaction conditions or with very apolar substrates. This ability enables, for example, catalysis in supercritical carbon dioxide as an alternative and environmentally friendly solvent,^[2] applications in biphasic mixtures for efficient catalyst recovery^[3] or selective reagent separation,^[4] and catalyst heterogenization and new delivery methods.^[5] Strategies to make a catalyst "fluorous" are versatile and perfluorinated groups can also be placed in the structure of a catalyst precursor to enhance its activation and reactivity through its miscibility in different phases.^[6] Fluorous catalysts in general show a versatile solubility behavior and are not limited to applications in equally fluorous solvents, which are often not desired because of their costs and environmental persistence.^[7]

[*] M. Schnitte, J. S. Scholliers, K. Riedmiller, Prof. Dr. S. Mecking
Chair of Chemical Materials Science, Department of Chemistry,
University of Konstanz
78457 Konstanz (Germany)
E-mail: stefan.mecking@uni-konstanz.de

Supporting information and the ORCID identification number(s) for the author(s) of this article can be found under:
<https://doi.org/10.1002/anie.201913117>.

© 2019 The Authors. Published by Wiley-VCH Verlag GmbH & Co. KGaA. This is an open access article under the terms of the Creative Commons Attribution Non-Commercial License, which permits use, distribution and reproduction in any medium, provided the original work is properly cited, and is not used for commercial purposes.

In contrast to their extensive utilization for solubility, examples where perfluorinated alkyl groups control the active metal center's catalytic reactivity are rare.^[8] Although their synthetic chemistry is well established their potential is largely unexplored in this regard.

We now report a case study showing how perfluoroalkyl substituents enhance catalyst performance. As a catalyst system, which is both mechanistically instructive to unravel the role of the perfluoroalkyl substituents, as well as practically useful, neutral Ni^{II} polymerization catalysts were studied.^[9]

Results and Discussion

Perfluoroalkyl-substituted (e.g. *n*-C₆F₁₃) *N*-terphenyl salicylaldiminato Ni^{II} catalysts (Figure 1) were recently demonstrated to be uniquely capable of a truly living polymerization of ethylene under aqueous conditions.^[10] In this process narrow distributed ultra-high-molecular-weight strictly linear polyethylene (UHMWPE) is generated, in the unusual form of monodisperse uniformly shaped nanocrystals.

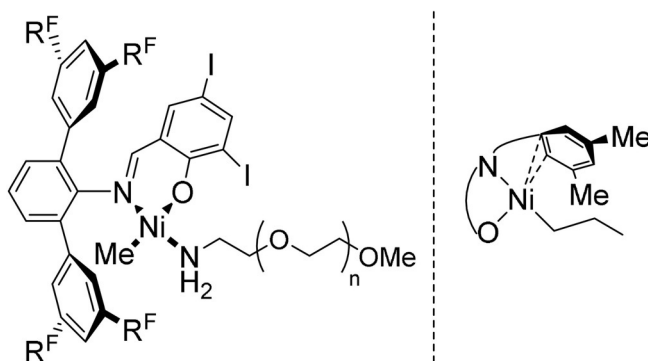


Figure 1. Catalyst precursor, with C₆F₁₃-substituents at remote positions, capable of truly living ethylene polymerization in aqueous media (left).^[10] Interaction promoting chain transfer and branch formation in the case of electron-donating substituents, exemplified by methyl substituents (right).^[11]

The strong influence of substituents at these remote positions of the chelating ligand, distant from the active center, can be related to a weak interaction between the distal aryl rings and the metal atom (Figure 1, right), and it promotes decoordination of ethylene and favors β -hydride elimination (BHE).^[11] BHE is the key step in chain transfer and branch formation. This weak interaction is promoted by electron-donating groups, which afford hyperbranched ethyl-

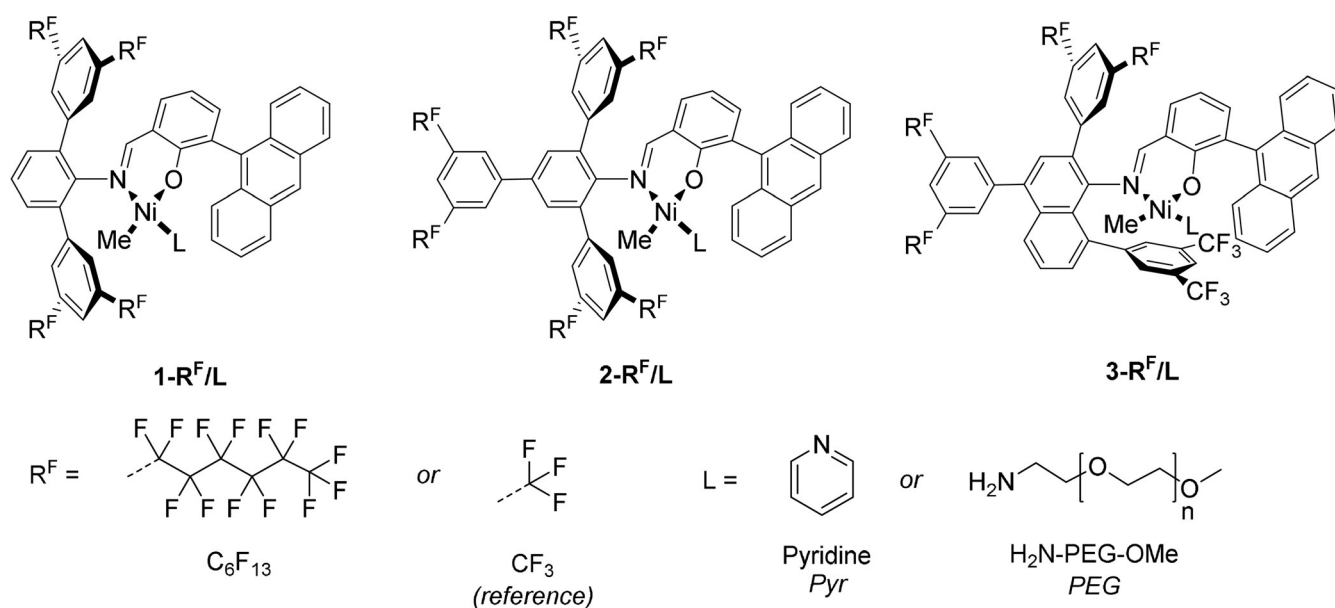


Figure 2. Catalyst precursors studied in this work. Compared to the reference systems ($R^F = CF_3$), the novel catalysts are substituted with linear long perfluoroalkyl groups ($R^F = C_6F_{13}$) in remote positions. The coordinated labile ligand L differs for lipophilic precursors ($L = Pyr$) and hydrophilic precursors ($L = PEG$) suitable for aqueous polymerizations.

ene oligomers. In contrast, with electron-withdrawing trifluoromethyl groups linear polyethylene is formed under otherwise identical conditions.^[12,13] Note that an H–F interaction with the growing chain, which was suggested for early^[14] and late-transition-metal catalysts,^[15] is clearly not operative.^[16]

To understand their role in catalysis, we investigated the influence of long perfluoroalkyl substituents (linear C_6F_{13} groups) in different established salicylaldiminato Ni^{II} motifs under a set of polymerization reaction conditions. We targeted the *N*-(quar)terphenyl-based **1-R^F/L** and **2-R^F/L** (Figure 2), known to be active in aqueous and nonaqueous ethylene polymerization to linear high-molecular-weight polyethylene.^[13,17–19] We also modified the *N*-naphthyl-type catalyst **3-R^F/L** (Figure 2), capable of a controlled/living ethylene polymerization in a variety of solvents, and introduced C_6F_{13} -substituents to selected positions.^[20] Anthryl moieties were placed in close proximity to the nickel center to shield the axial site and impede chain-transfer reactions.^[13,21]

The synthesis of the respective salicylaldimines was straightforward according to known procedures, slightly modified to handle the highly lipophilic intermediate products (see the Supporting Information for details of synthesis and characterization of all catalyst precursors). As a key step, a copper-promoted Ullmann coupling of 1,3-diiodobenzene and perfluorohexyl iodide provided access to the 1,3-(diperfluorohexyl)phenyl motif incorporated into the aforementioned catalyst structures. Lipophilic precatalysts were obtained by reaction of salicylaldimines with $[(tmeda)NiMe_2]$ in the presence of pyridine as a labile ligand. Hydrophilic analogues, suitable for aqueous polymerizations, were obtained in the presence of α -methoxy- ω -amino poly(ethylene glycol) (H_2N -PEG-OMe, Figure 2).

Ethylene polymerization studies in heptane were carried out at different temperatures (30–50 °C), with C_6F_{13} -substituted catalyst precursors and the analogous CF_3 complexes to identify the effects of the perfluoroalkyl substituent under lipophilic conditions (Table 1). All catalysts studied were active in ethylene polymerization and a significant effect of the perfluoroalkyl chain length on catalytic performance and polymer properties was observed. Compared to their CF_3 analogues, the C_6F_{13} -substituted catalysts **1- C_6F_{13} /Pyr** and **2- C_6F_{13} /Pyr** showed higher activities ($15 \times 10^3 TOh^{-1}$ vs. $35 \times 10^3 TOh^{-1}$, entries 1 and 2) and produced narrower distributed polyethylene of higher molecular weights ($167 \times 10^3 g mol^{-1}$ vs. $504 \times 10^3 g mol^{-1}$, entries 1 and 2) with fewer branches (2.3 vs. < 1.0 branches per 1000 carbon atoms, entries 1 and 2) at a reaction temperature of 30 °C. Chain transfer (which limits molecular weight and broadens molecular weight distribution) and branch formation proceed through BHE. The above data indicates a very effective suppression of these pathways by the C_6F_{13} substitution. Similar trends of activity and branching were observed at a higher reaction temperature of 50 °C when comparing **1- CF_3 /Pyr** and **1- C_6F_{13} /Pyr** and **2- CF_3 /Pyr** and **2- C_6F_{13} /Pyr**.

In the case of the **3-R^F/Pyr** catalysts, the **3- C_6F_{13} /Pyr** produced polyethylene with fewer branches. Other than this, no significant differences were observed. Both catalysts perform a highly controlled polymerization as indicated by the chains per nickel ratios being close to unity and the narrow molecular weight distributions of $M_w/M_n = 1.2$.

The observed increase in polymerization rate and molecular weights for the C_6F_{13} -substituted catalysts versus the CF_3 reference, together with a decrease in branching indicate a significant influence of the perfluoroalkyl substituents, at remote positions of the catalyst structures, on the active nickel center. To further illuminate the origin of this effect, cyclic

Table 1: Ethylene polymerization experiments in heptane.

Entry	Precatalyst	$E_1^{[a]}$ [mV]	T [°C]	Yield PE [g]	TOF ^[b]	$M_n^{[c]}$ [10^3 g mol ⁻¹]	$M_w/M_n^{[c]}$	Chains/[Ni]	$T_m^{[d]}$ [°C] (Cryst. [%])	Branches/1000 C ^[e]
1	1-CF ₃ /Pyr	254	30	0.68	14.6	167	1.9	0.8	134 (53)	2.3
2	1-C ₆ F ₁₃ /Pyr	560	30	1.66	35.3	504	1.6	0.7	133 (49)	<1.0
3	1-CF ₃ /Pyr	254	50	2.28	48.8	80	3.3	5.7	124 (47)	12.4
4	1-C ₆ F ₁₃ /Pyr	560	50	5.68	121.4	82	2.9	13.8	124 (50)	8.4
5	2-CF ₃ /Pyr	329	30	0.99	21.2	91	2.4	2.2	136 (57)	4.7
6	2-C ₆ F ₁₃ /Pyr	445	30	1.33	28.4	294	1.6	0.9	133 (55)	2.9
7	2-CF ₃ /Pyr	329	50	2.68	57.3	82	4.6	6.6	125 (51)	17.8
8	2-C ₆ F ₁₃ /Pyr	445	50	5.23	111.8	77	2.5	13.6	123 (49)	13.4
9	3-CF ₃ /Pyr	357	50	1.40	50.0	618	1.2	0.8	135 (47)	3.7
10	3-C ₆ F ₁₃ /Pyr	395	50	1.24	44.2	683	1.2	0.6	135 (46)	<1.0

Reaction conditions: 5 μ mol catalyst loading, 20 minutes reaction time, 40 bar ethylene pressure, in 100 mL heptane. [a] Determined by cyclic voltammetry. [b] Given in $10^3 \times \text{mol} [\text{C}_2\text{H}_4] \times \text{mol}^{-1} [\text{Ni}] \times \text{h}^{-1}$. [c] Determined by GPC at 160 °C. [d] Determined by DSC (heating rate: 10 K min⁻¹); second heating cycle reported. [e] Determined by selective detection of methyl and methylene IR-bands during GPC measurements (versus standards with known degree of branching).

voltammetry experiments were performed on all pyridine precatalysts. The observed oxidation and reduction transitions for the Ni^{II}/Ni^{III} pair showed that compared to the reference trifluoromethyl catalysts, the electron density at the metal center is significantly lower in the C₆F₁₃-substituted complexes as evidenced by an increase in measured forward peak potentials (column E_1 , Table 1) found for all catalyst types studied. This remarkable decrease in electron density (e.g. 211 mV [$R^F = \text{CF}_3$] vs. 541 mV [$R^F = \text{C}_6\text{F}_{13}$] for **1-R^F/Pyr**, Table 1) correlates qualitatively with the observed catalytic and polymer properties in case of catalyst types **1-R^F/Pyr** and **2-R^F/Pyr** (Figure 3). Note, that this effect on polymer microstructure may be enhanced further by the higher steric demand^[22] of perfluoroalkyl versus trifluoromethyl substituents.

For catalyst types **3-R^F/Pyr**, only a small difference in forward peak potentials was observed (357 mV [$R^F = \text{CF}_3$] vs. 395 mV [$R^F = \text{C}_6\text{F}_{13}$], entries 9 and 10, Table 1). This reduced effect of the substitution pattern compared to the other two types of catalysts is expected given that only one of the aryl substituents in *o*-position of the N-phenyl group is altered, and the phenyl ring closest to the nickel center (8-position of the naphthylamine moiety, Figure 2) was not modified. This electrochemical data agrees well with similar catalytic properties observed for **3-C₆F₁₃/Pyr** and **3-CF₃/Pyr** (Table 1), with the C₆F₁₃-substitution leading to a slight decrease in branching only while catalytic activity and molecular weight are similar to the CF₃ analogue.

To probe for any pronounced solvent effects, for example through interactions with the active site or by the solvent quality for the polymer product formed, we performed polymerization experiments in toluene as a somewhat more polar and aromatic solvent (see the Supporting Information for comprehensive experimental and analytical data of polymerization experiments in toluene with all catalyst precursors at different temperatures). In summary, we observed the same trends for **1-R^F/Pyr** and **2-R^F/Pyr** as outlined above, with a superior role of catalysts with long perfluoroalkyl substituents. Namely, compared to the CF₃ reference 1) increased molecular weights (240×10^3 g mol⁻¹ vs. 623×10^3 g mol⁻¹; see Table S1, entries 1 and 2 in the Supporting Information); 2) slightly increased catalytic activ-

ities (61×10^3 TOh⁻¹ vs. 73×10^3 TOh⁻¹; Table S1, entries 1 and 2); and 3) decreased degrees of branching (1.7 vs. 1.1 branches per 1000 carbon atoms; Table S1, entries 1 and 2) were found. In line with the above polymerizations in heptane and cyclic voltammetry experiments, no significant impact of the longer perfluoroalkyl substituents in catalysts **3-R^F/Pyr**

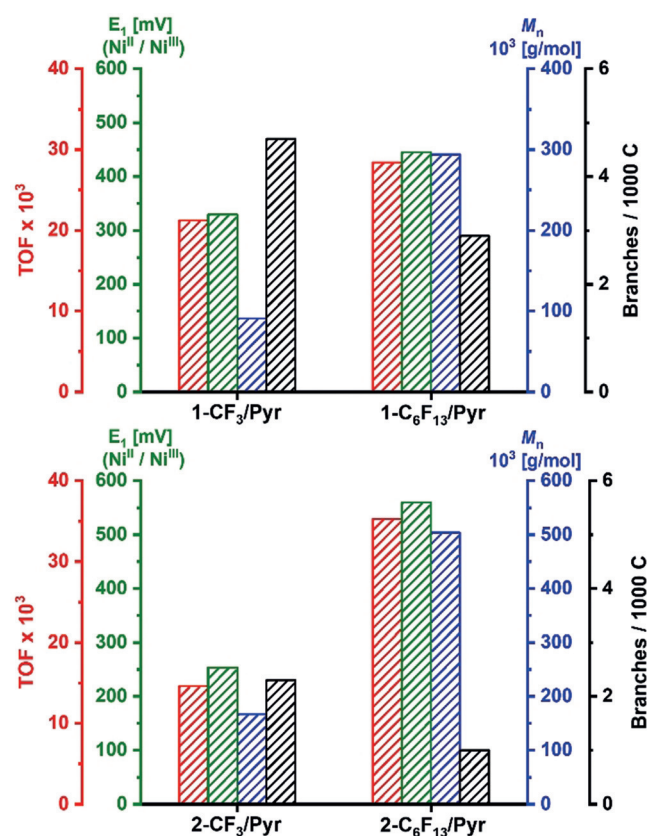


Figure 3. Comparison of experimental polymerization data with cyclic voltammetry data for different catalyst precursors (**1-R^F/Pyr**, top and **2-R^F/Pyr**, bottom). Catalytic activity (TOF, red), forward peak potential determined by cyclic voltammetry (E_1 , green), molecular weight (blue), and branching values (black) of polyethylenes formed versus different catalyst precursors given. Experimental data from experiments at 30 °C in heptane (entries 1, 2, 5, and 6, Table 1).

was observed. **3-C₆F₁₃/Pyr** produced polyethylene with slightly lower activity and, accordingly, with slightly lower molecular weights.

The high functional-group tolerance of late-transition-metal catalysts allows their use even in polar protic environments.^[23] During polymerization in aqueous surfactant solution with Ni^{II} salicylaldiminato catalysts, the polyethylene is formed in the very unusual form of nanoscale single crystals.^[17] They are characterized by a high degree of order, which arises from the unique particle growth mechanism, where the active center's growing chain is directly deposited on the crystal growth front, leaving no opportunity for any disorder.^[18,24] This process allows effective generation of anisotropic polymer nanoparticles, which are otherwise difficult to access.^[25]

All hydrophilic catalyst precursors of types **1-R^F**, **2-R^F**, and **3-R^F** (with H₂N-PEG-OMe as labile ligand) were active for several hours under established reaction conditions in water (Table 2). Remarkably, all C₆F₁₃-substituted catalysts studied are clearly superior in aqueous polymerization compared to their CF₃ analogues, in terms of catalytic activities and properties of the produced polyethylenes. In the case of **1-C₆F₁₃/PEG** and **2-C₆F₁₃/PEG**, the perfluoroalkyl substitution led to a comparable substantial increase in catalytic activities (e.g. 23 × 10³ TO vs. 51 × 10³ TO, entries 3 and 4), molecular weights (484 × 10³ g mol⁻¹ vs. 866 × 10³ g mol⁻¹, entries 1 and 2), and decreased polydispersities (2.0 vs. 1.3, entries 1 and 2), and branch contents (1.6 vs. < 1.0 branches per 1000 carbon atoms, entries 1 and 2) versus the trifluoromethyl reference. Under optimized reaction conditions (10 °C reaction temperature, high surfactant loading), both **1-C₆F₁₃/PEG** and **2-C₆F₁₃/PEG** are capable of a truly living ethylene polymerization in water, as evidenced by 1) linear relationships between yields and molecular weights; 2) narrow molecular weight distributions of M_w/M_n < 1.3; and 3) chain per nickel ratios close to unity (see Tables S2 and S3 for comprehensive experimental and analytical data; Figure 4). Even linear and narrow distributed UHWMPE with M_n = 2.0 × 10⁶ g mol⁻¹ is

accessible at extended reaction times, as one nickel center grows one polymer chain over the entire polymerization experiment.

Likewise, **3-C₆F₁₃/PEG** stands out as the first reported N-naphthyl-type nickel(II) salicylaldiminato catalyst with adequate activities in water and accessible molecular weights of M_n = 1.6 × 10⁶ g mol⁻¹ with very narrow distributions of M_w/M_n = 1.1 in a strictly living polymerization (see Table S4 for comprehensive experimental and analytical data; Figure 4). Different from the nonaqueous polymerization with catalyst motif **3-R^F**, in the aqueous polymerization the CF₃ analogue is much less active (45 × 10³ TO vs. 8 × 10³ TO; Table 2, entries 5 and 6) and less controlled compared to the perfluoroalkyl complex. As polymerizations under aprotic conditions and insights from cyclic voltammetry experiments did not suggest a significant electronic influence of the long perfluoroalkyl groups on the active center for this catalyst type **3-R^F**, we tentatively address this different behavior in the aqueous system to the highly hydrophobic groups on the salicylaldiminato ligand. Possibly, the four C₆F₁₃ substituents create a highly apolar environment around the metal center, which promotes rapid dissociation of the hydrophilic polar labile H₂N-PEG-OMe ligand into the aqueous solution and allows an effective catalyst activation. ¹H NMR spectra of catalysts **3-R^F/PEG** point to a very strong binding of the labile ligand to the nickel center, as indicated by a hindered rotation (diastereotopic character) of the amino functionality and the protons in α- and β-positions (see Figures S10, S12, and S15), which might prohibit an effective activation for the catalyst with exclusively trifluoromethyl substituents.

Considering the particle formation process, the generation of very small (< 100 nm) particles requires a high degree of dispersion of the catalyst precursor,^[26] and under ideal conditions an entire particle is grown by a single active site.^[10] With the catalysts studied here, stable dispersions with a single well-defined particle population were obtained as observed by DLS (Figure 5). Even these highly fluorinated catalysts (e.g. 36 perfluorinated carbon atoms in chemical structure of

Table 2: Ethylene polymerization experiments in aqueous surfactant solution.

Entry	Precatalyst	Yield PE [g]	TON ^[a]	M _n ^[b] [10 ³ g mol ⁻¹]	M _w /M _n ^[b]	Chains/[Ni]	T _m ^[c] [°C] (Cryst. [%])	Branches/1000 C ^[d]	d _h (Vol.) ^[e] [nm]
1	1-CF ₃ /PEG	5.87	27.9	484	2.0	1.6	142 (55)/ 135 (36) 134	1.6	22 (0.05)
2	1-C ₆ F ₁₃ /PEG	9.61	45.7	866	1.3	1.5	143 (73)/ 135 (48) 133	< 1.0	25 (0.08)
3	2-CF ₃ /PEG	4.78	22.7	408	1.8	1.6	140 (66)/ 135 (49) 134	< 1.0	23 (0.07)
4	2-C ₆ F ₁₃ /PEG	10.65	50.6	885	1.4	1.6	140 (64)/ 133 (41) 133	< 1.0	31 (0.12)
5	3-CF ₃ /PEG	1.64	7.8	486	1.6	0.5	138 (63)/ 135 (51) 134	2.6	16 (0.14)
6	3-C ₆ F ₁₃ /PEG	9.39	44.6	1609	1.2	0.8	142 (65)/ 136 (41) 137	< 1.0	21 (0.17)

Reaction conditions: 7.5 μmol catalyst loading, 40 bar ethylene pressure, 4 hours reaction time, 15 °C reaction temperature, 6.0 g sodium dodecyl sulfate, 1.5 g cesium hydroxide, 0.75 mL mesitylene, in 150 mL degassed water, ultrasound applied prior to ethylene pressurization. [a] Given in 10³ × mol [C₂H₄]/mol [Ni]. [b] Determined by GPC at 160 °C. [c] Determined by DSC; reported as [first heating cycle (crystallinity)]\2nd heating cycle (crystallinity)] with 10 K min⁻¹ heating rate, second line: first heating cycle with 1 K min⁻¹ heating rate. [d] Determined by selective detection of methyl and methylene IR-bands during GPC measurements (calibrated versus samples with known degree of branching). [e] Determined by DLS; volume mean and PDI reported.

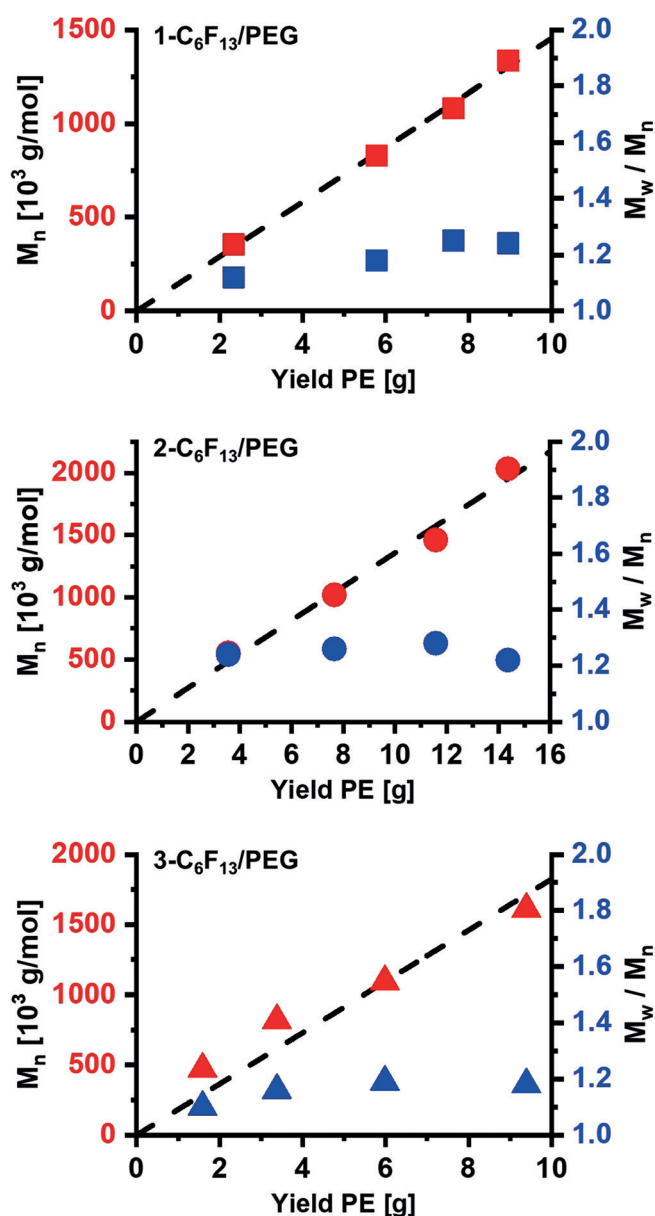


Figure 4. Molecular weights and polydispersity indices of polyethylenes versus yields from different aqueous polymerizations with different catalyst precursors (see Tables S2–S4 for comprehensive experimental and analytical data).

2- C_6F_{13} /PEG) are able to form small uniform particles under aqueous conditions, which are composed of completely disentangled polyethylene chains as evidenced by high melting points in the first heating cycle with low melting points observed for slow heating rates.^[27]

Conclusion

In summary, we present a clear case demonstrating the utility of perfluoroalkyl substituents to control catalytic properties. This utility demonstrates their potential for catalysis beyond the established use for achieving solubility in very apolar and fluoruous media. The C_6F_{13} groups in the

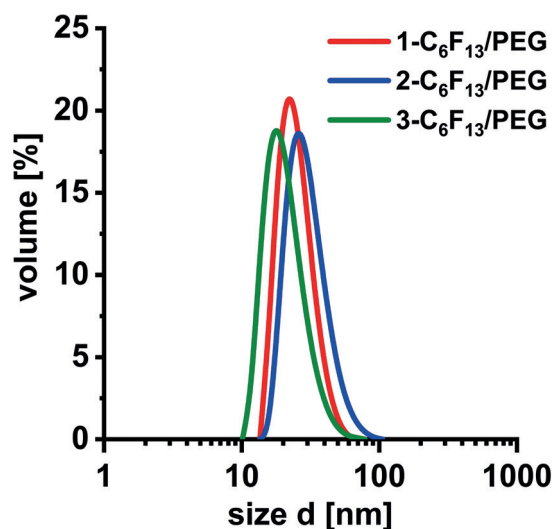


Figure 5. DLS traces of polyethylene dispersions obtained from aqueous polymerization with different catalyst precursors (Table 2, entries 2, 4, and 6).

catalyst motifs studied substantially increased catalyst activity and molecular weight of the polymer product, and reduced branching. This observation establishes the mechanistic picture of a reduced electron density on the active metal sites—also supported by cyclic voltammetry on the catalyst precursors—when compared to the more commonly used trifluoromethyl groups. For the catalytic chain growth polymerization studied here, the C_6F_{13} group favors chain growth and disfavors BHE, which is the key step of undesired chain transfer and branching pathways. This suppression of chain transfer occurs to an extent that enables truly living polymerizations even in aqueous systems. Perfluoroalkyl groups are similarly or slightly more electron withdrawing compared to CF_3 groups.^[28] This character accounts for their beneficial impact observed here. Further, longer substituents in the remote positions of the *o*-terphenyl motif also reduce BHE,^[22] possibly by hindering conformations suitable for an aryl-Ni interaction.

Experimental Section

Experimental Details are described in detail in the Supporting Information.

Acknowledgements

Financial support by the DFG (SFB 1214) is gratefully acknowledged. We thank Anke Friemel for NMR measurements and Sonja Stadler for a sample of 2- CF_3 /Pyr. We thank Larissa Casper from the group of Rainer Winter for support with cyclic voltammetry experiments.

Conflict of interest

The authors declare no conflict of interest.

Keywords: homogeneous catalysis · fluorine · ligand design · nickel · polymers

How to cite: *Angew. Chem. Int. Ed.* **2020**, *59*, 3258–3263
Angew. Chem. **2020**, *132*, 3284–3289

-
- [1] V. H. Dalvi, P. J. Rossky, *Proc. Natl. Acad. Sci. USA* **2010**, *107*, 13603–13607.
- [2] a) S. Kainz, D. Koch, W. Leitner, W. Baumann, *Angew. Chem. Int. Ed. Engl.* **1997**, *36*, 1628–1630; *Angew. Chem.* **1997**, *109*, 1699–1701; b) Y. Hu, W. Chen, A. M. B. Osuna, J. Xiao, A. M. Stuart, E. G. Hope, *Chem. Commun.* **2001**, 725–726; c) A. Bastero, G. Franciò, W. Leitner, S. Mecking, *Chem. Eur. J.* **2006**, *12*, 6110–6116.
- [3] J. A. Gladysz, R. Corrêa da Costa in *Handbook of fluororous chemistry* (Eds.: J. A. Gladysz, D. P. Curran, I. T. Horváth), Wiley-VCH, Weinheim, **2004**, pp. 24–40.
- [4] a) S. G. Leach, C. J. Cordier, D. Morton, G. J. McKiernan, S. Warriner, A. Nelson, *J. Org. Chem.* **2008**, *73*, 2753–2759; b) D. Morton, S. Leach, C. Cordier, S. Warriner, A. Nelson, *Angew. Chem. Int. Ed.* **2009**, *48*, 104–109; *Angew. Chem.* **2009**, *121*, 110–115.
- [5] a) J. Lim, S. S. Lee, J. Y. Ying, *Chem. Commun.* **2008**, 4312–4314; b) L. V. Dinh, J. A. Gladysz, *Angew. Chem. Int. Ed.* **2005**, *44*, 4095–4097; *Angew. Chem.* **2005**, *117*, 4164–4167.
- [6] a) S. K. Ghosh, A. S. Ojeda, J. Guerrero-Leal, N. Bhuvanesh, J. A. Gladysz, *Inorg. Chem.* **2013**, *52*, 9369–9378; b) Z. Xi, H. S. Bazzi, J. A. Gladysz, *J. Am. Chem. Soc.* **2015**, *137*, 10930–10933.
- [7] a) A. R. Ravishankara, S. Solomon, A. A. Turnipseed, R. F. Warren, *Science* **1993**, *259*, 194–199; b) C. C. Tzschucke, C. Markert, H. Glatz, W. Bannwarth, *Angew. Chem. Int. Ed.* **2002**, *41*, 4500–4503; *Angew. Chem.* **2002**, *114*, 4678–4681; c) M. Wende, R. Meier, J. A. Gladysz, *J. Am. Chem. Soc.* **2001**, *123*, 11490–11491.
- [8] a) S. Solyntjes, B. Neumann, H.-G. Stammler, N. Ignat'ev, B. Hoge, *Chem. Eur. J.* **2017**, *23*, 1568–1575; b) R. Mundil, A. Sokolohorskyj, J. Hošek, J. Cvačka, I. Čiřařová, J. Kvíčala, J. Merna, *Polym. Chem.* **2018**, *9*, 1234–1248; c) H. Jiao, S. Le Stang, T. Soós, R. Meier, K. Kowski, P. Rademacher, L. Jafarpour, J.-B. Hamard, S. P. Nolan, J. A. Gladysz, *J. Am. Chem. Soc.* **2002**, *124*, 1516–1523.
- [9] a) H. Mu, L. Pan, D. Song, Y. Li, *Chem. Rev.* **2015**, *115*, 12091–12137; b) C. Chen, *Nat. Rev. Chem.* **2018**, *2*, 6–14.
- [10] M. Schmitte, A. Staiger, L. A. Casper, S. Mecking, *Nat. Commun.* **2019**, *10*, 2592.
- [11] L. Falivene, T. Wiedemann, I. Göttker-Schnetmann, L. Caporaso, L. Cavallo, S. Mecking, *J. Am. Chem. Soc.* **2018**, *140*, 1305–1312.
- [12] M. A. Zuideveld, P. Wehrmann, C. Rohr, S. Mecking, *Angew. Chem. Int. Ed.* **2004**, *43*, 869–873; *Angew. Chem.* **2004**, *116*, 887–891.
- [13] I. Göttker-Schnetmann, P. Wehrmann, C. Röhr, S. Mecking, *Organometallics* **2007**, *26*, 2348–2362.
- [14] a) H. M. Möller, M. C. Baier, S. Mecking, E. P. Talsi, K. P. Bryliakov, *Chem. Eur. J.* **2012**, *18*, 848–856; b) M. Mitani, T. Nakano, T. Fujita, *Chem. Eur. J.* **2003**, *9*, 2396–2403.
- [15] M. P. Weberski, C. Chen, M. Delferro, C. Zuccaccia, A. Macchioni, T. J. Marks, *Organometallics* **2012**, *31*, 3773–3789.
- [16] A. Osichow, I. Göttker-Schnetmann, S. Mecking, *Organometallics* **2013**, *32*, 5239–5242.
- [17] I. Göttker-Schnetmann, B. Korthals, S. Mecking, *J. Am. Chem. Soc.* **2006**, *128*, 7708–7709.
- [18] A. Osichow, C. Rabe, K. Vogtt, T. Narayanan, L. Harnau, M. Drechsler, M. Ballauff, S. Mecking, *J. Am. Chem. Soc.* **2013**, *135*, 11645–11650.
- [19] P. Kenyon, S. Mecking, *J. Am. Chem. Soc.* **2017**, *139*, 13786–13790.
- [20] a) P. Kenyon, M. Wörner, S. Mecking, *J. Am. Chem. Soc.* **2018**, *140*, 6685–6689; b) Z. Chen, M. Mesgar, P. S. White, O. Daugulis, M. Brookhart, *ACS Catal.* **2015**, *5*, 631–636.
- [21] a) L. K. Johnson, C. M. Killian, M. Brookhart, *J. Am. Chem. Soc.* **1995**, *117*, 6414–6415; b) T. R. Younkin, E. F. Conner, J. I. Henderson, S. K. Friedrich, R. H. Grubbs, D. A. Bansleben, *Science* **2000**, *287*, 460–462.
- [22] T. Wiedemann, G. Voit, A. Tchernook, P. Roesle, I. Göttker-Schnetmann, S. Mecking, *J. Am. Chem. Soc.* **2014**, *136*, 2078–2085.
- [23] a) A. Nakamura, S. Ito, K. Nozaki, *Chem. Rev.* **2009**, *109*, 5215–5244; b) M. R. Radlauer, A. K. Buckley, L. M. Henling, T. Agapie, *J. Am. Chem. Soc.* **2013**, *135*, 3784–3787.
- [24] A. Godin, I. Göttker-Schnetmann, S. Mecking, *Macromolecules* **2016**, *49*, 8825–8837.
- [25] a) D. J. Walsh, D. Guironnet, *Proc. Natl. Acad. Sci. USA* **2019**, *116*, 1538–1542; b) C. E. Boott, J. Gwyther, R. L. Harniman, D. W. Hayward, I. Manners, *Nat. Chem.* **2017**, *9*, 785–792.
- [26] C. Boucher-Jacobs, M. Rabnawaz, J. S. Katz, R. Even, D. Guironnet, *Nat. Commun.* **2018**, *9*, 841.
- [27] S. Rastogi, D. R. Lippits, G. W. H. Höhne, B. Mezari, P. C. M. M. Magusin, *J. Phys. Condens. Matter* **2007**, *19*, 205122.
- [28] a) C. Hansch, A. Leo, R. W. Taft, *Chem. Rev.* **1991**, *91*, 165–195; b) J. A. Gladysz in *Handbook of fluororous chemistry* (Eds.: J. A. Gladysz, D. P. Curran, I. T. Horváth), Wiley-VCH, Weinheim, **2004**, pp. 41–55.

Manuscript received: October 14, 2019

Revised manuscript received: November 26, 2019

Accepted manuscript online: November 27, 2019

Version of record online: January 21, 2020